TOWARDS QUANTUM GRAVITY: DISCRETE GEOMETRY – OBSERVABLE CONSEQUENCES

SETH A. MAJOR

ABSTRACT. This is an extended set of lecture notes of a talk at Swarthmore College in March 1999. The Hamiltonian approach to quantum gravity is reviewed with a focus on some conceptual issues, spin network diagrammatics, and two possible arenas for observation of quantum gravitational phenomenon.

1. INTRODUCTION

Today I wish to tell you about a promising attempt to combine two developments in twentieth century physics, general relativity and quantum theory. Progress on this problem has been simmering along on a back burner since the 1920's, eclipsed in part due to the remoteness of its expected range of applicability. Here I hope to motivate why one would undertake such a study, present some of the results in this study, and explain ways in which the quantum effects of gravitation could manifest themselves in observable ways.

Both theories are great departures from classical physics. In general relativity, space and time combined to give the single, dynamical entity of spacetime. Simple statements as, "Two particles are a distance r apart at time t." become meaningless. Such concepts as local energy density of the gravitational field elude definition. In quantum theory we loose the notion of assigning definite values to observables. Also in quantum theory physical quantities may no longer commute, xp^2 is no longer equal to pxp. This vast new freedom means that there are many quantum theories for every classical one; when quantizing one is faced with many choices. Classical theories have no need for a well-defined quantum limit. They may be oblivious to it. Thus when "going the wrong way," from a classical theory to quantum one, it as if one is climbing a tree in the dark, going from trunk to twig, trying to find the branch with an Easter egg – the correct physical theory. At each choice one doesn't know a priori which turn will lead to the correct space.

The approach I'll talk about here is be a conservative one, "Take general relativity and quantize it." But it is also a radical approach. Since there is no way to define distance without the metric one needs a background-independent quantization – entirely new for quantum theory. The strategy is familiar, first study the kinematics, then turn to the dynamics. The present status of this quantization is that the kinematics is largely formulated, though there is much to understand, but the dynamics remains controversial. There is a good review in Ref. [20], though it assumes a fair amount of background.

In what regime might this theory be valid? To put it dramatically, every good theory carries the seed of its own destruction. To put it more accurately, from every good theory one can derive its range of validity. As an example, let's do a calculation which Laplace performed two hundred years ago. It is something we might use to fill up the margins of our mechanics textbooks. In the chapter on gravitation. Is there a situation in which even light doesn't have enough speed to escape a potential well? More precisely, if we had a test mass moving very near

the speed of light, is there a system from which it cannot escape? In general, to find escape velocity we need to find the kinetic energy needed to climb out of the gravitational potential

$$\frac{mv_{esc}^2}{2r} = \frac{GmM}{r}$$

If our test mass can not escape – $v_{esc} = c$ – then the escape velocity equation can be used to give a distance R_S[1]

(1)
$$R_S = \frac{2GM}{c^2}$$

which is now called, not the Laplace radius, but the Schwarschild radius after the person who found the spherically symmetric solution to Einstein's equations. This calculation is not "a seed of destruction" for Newtonian theory – we found a reasonable answer – but rather gives a justifiably special radius (when c is finite).

To find the expected scale of the theory of quantum gravity we can perform a very simple calculation: Something new ought to happen when a massive particle's Compton wavelength and Schwarschild radius of Eq. (1) become equal, i.e. when

$$\frac{h}{mc} = \frac{2Gm}{c^2}$$

or, at the Planck scale

$$m_p = \sqrt{\frac{hc}{G}} \approx 10^{19} \text{ GeV} \approx 10^9 \text{J}$$

In fact it was Planck of Planck's constant who first wrote down this relation and the distance scale

$$l_p = \sqrt{\frac{G\hbar}{c^3}} \approx 10^{-35}\text{m}$$

– a distance scale far below anything that we could expect to directly access with experiments. In terms of modern accelerators which operate at 10^3 GeV this is unobservable. There are 19 orders of magnitude between the Planck scale and the scales tested by present day accelerators. In fact, using accelerators to test quantum gravity would be like using soccer matches to find the mass of the top quark!

If not here on Earth, perhaps astronomical observations could provide a realm of quantum gravity. Perhaps the first objects to come to mind are black holes. But these are object from which "nothing can escape." This makes directly observing them difficult. However there is strong, indirect evidence that the universe is populated with these beasts. Perhaps the best is from a set of observations of galactic nuclei. The first observations were with radio data of water masers in NGC 4258 [15]. Using radiation from matter orbiting a central, supermassive object they were able to measure the Doppler shift in radiation from the orbit and thus were able to find the velocity. With the radius of the orbit they were able to find the mass of the nucleus, 3.6×10^7 solar masses. The most likely candidate is a black hole.

In the remainder of this talk will be to describe quantum gravity phenomenon, one related to black holes, the other arising from the microstructure of spacetime. To do this I will first need to describe the scenery. The first section will be on properties of black holes. The second will be on quantum gravity itself, by way of a new way of looking at the familiar angular momentum operators of quantum

---

[1]This calculation ought to be treated with some care. For instance, it does not imply that light released from a massive object would climb to a height equal to the Schwarschild radius and then fall back towards the surface. This calculation merely gives a result which, when placed in the context of general relativity, yields radius of the horizon.

mechanics. In the final section I return to black holes and possible experimental observations.

2. BLACK HOLES AND THERMODYNAMICS

In the early seventies there was a flurry of new results about black holes. These were often given in mathematically rigorous terms and are collectively known as "Black Hole Mechanics." I will summarize these for neutral, time-independent, (the technical term is "stationary") non-rotating black holes (though all this goes through for black holes with charge and angular momentum).

Let me first give a brief summary of the geometry. Schwarschild black holes have many wild and wonderful properties but I will concentrate on just a few. The metric – used to measure the length and duration between events – on the spacetime is

$$ds^2 = -\left(1 - \frac{2GM}{c^2 r}\right) dt^2 + \left(1 - \frac{2GM}{c^2 r}\right)^{-1} dr^2 + r^2 d\theta^2 + r^2 \sin^2 \theta \, d\phi^2$$

Two aspects of this metric call our attention. Something fishy happens at $r = 0$ and at $r = \frac{2GM}{c^2}$. It turns out that only at $r = 0$ is there a nasty singularity. The "apparent singularity" at $r = \frac{2GM}{c^2}$ is an artifact of the coordinates. However, as we see from Laplace's calculation this radius is nevertheless important. It identifies the horizon beyond which light (and thus, classically, everything) cannot escape. A nice way to think about horizons is to identify them with the boundary between the region in which light rays climb out of a gravitational well and the region in which light rays fall into the singularity at $r = 0$. While an observer will not notice anything unusual while passing through the horizon, It was only realized relatively recently that it may not be the central singularity which is as important as the fact that such objects come with horizons. The horizon has an area

$$(2) \qquad A_{\mathcal{H}} = 4\pi R_S^2 = \frac{16\pi G^2}{c^4} M^2$$

On this horizon there is a quantity κ called "surface gravity" which is likened (but somewhat misleadingly!) to little g of Newtonian gravity. It is the force that a distant observer would exert on a unit test mass to hold it at the horizon.

Law	Thermodynamics	Black Holes
0	T is constant throughout body in thermal equilibrium	κ is constant over the horizon
1	$dU = TdS$ when $dW = 0$	$dM = \frac{1}{8\pi}\kappa \, dA_{\mathcal{H}}$
2	$dS \geq 0$ for any process	$dA_{\mathcal{H}} \geq 0$ for any process
3	$T = 0$ is not attainable by a physical process "$S \to 0$ as $T \to 0$"	$\kappa = 0$ is not attainable by a physical process

$(G = c = \hbar = k = 1$ in this table !)

Note that there is a mapping between the two:

$$
\begin{aligned}
U &\leftrightarrow M, \\
T &\leftrightarrow \frac{\kappa}{2\pi}, \text{ and} \\
S &\leftrightarrow A_{\mathcal{H}}/4
\end{aligned}
$$

(3)

does the trick.

Bekenstein first made an analogy between thermodynamics and black hole mechanics by finding that, when black hole entropy was related to area, then a "generalized second law of thermodynamics" held. Defining the total entropy as $S_T = S_{BH} + S_E$ with S_E being the entropy of the environment and

$$S_{BH} = \frac{1}{4} k \frac{A_{\mathcal{H}}}{l_p^2}$$

(k is the Boltzmann constant) for the entropy of the black hole the total entropy never decreases, $\delta S_T \geq 0$. This was based on classical analysis. However, Bekenstein did not complete the analogy in the sense that he did not identify the temperature of a black hole. Classically the black hole is a perfect absorber so one would expect that the temperature is zero. However, this suggestion of Bekenstein effectively required that there was a non-zero temperature.

The temperature was found by an incredulous Hawking who, while attempting to show that the generalized second law was ill-founded, managed to find that in the semiclassical regime black holes do emit a thermal distribution of particles. He found that the temperature of a stationary black hole was related to the surface gravity, κ, [10]

$$(4) \qquad T_H = \frac{\hbar c^3}{2\pi G k} \kappa = \frac{\hbar c^3}{2\pi G k} \frac{1}{4M} \approx 10^{-7} \left(\frac{M_\odot}{M} \right) \text{ with } \kappa = \frac{1}{4M}.$$

Black holes (in vacuum) are not black! They radiate a black body spectrum at temperature T_H. This completed the analogy. For each of the laws of thermodynamics, there is a corresponding law of black hole mechanics.

But there is a candidate theory of quantum spacetime. What does it say about the nature of the radiation from black holes? To answer this I must introduce a fun, new tool, spin networks, which also gives you a new way of looking at a (hopefully) familiar object – the angular momentum states of quantum mechanics.

3. Angular momentum representation:Diagrammatics

This is a matter of expressing the familiar results of angular momentum states in terms of diagrams, lines, loops, and operators. I begin with a "topological" diagrammatic algebra.

3.1. **Line, bend and loop.** The Kronecker δ_A^B is the 2×2 identity matrix in component notation. Thus,

$$\left(\delta_A^B \right) = \begin{pmatrix} 1 & 0 \\ 0 & 1 \end{pmatrix}$$

and $\delta_0^0 = \delta_1^1 = 1$ while $\delta_0^1 = \delta_1^0 = 0$. The Latin capital indices, A and B in this expression, may take one of two values 0 or 1.

The diagrammatics begins by associating the Kronecker δ to a line

$$\delta_A^B \sim \Big)_A^B .$$

The position of the indices on δ determines the location of the labels on the ends of the line. Applying the definitions one has

$$\Big)_1^1 = 1 \text{ and } \Big)_0^1 = 0.$$

If a line is the identity then it is reasonable to associate a curve to a matrix with two upper (or lower) indices. Here, there is some choice in definition. A particularly

nice one i.e. one with useful and fun properties is the antisymmetric matrix ϵ_{AB}

$$(\epsilon_{AB}) = (\epsilon^{AB}) = \begin{pmatrix} 0 & 1 \\ -1 & 0 \end{pmatrix}.$$

But with an extra i tossed in:

$$\tilde{\epsilon}_{AB} := i\epsilon_{AB} \sim \overset{\displaystyle \frown}{}_{\mathbf{A} \quad \mathbf{B}}.$$

Similarly,

$$\tilde{\epsilon}^{AB} := i\epsilon^{AB} \sim \overset{\mathbf{A} \quad \mathbf{B}}{\underset{\displaystyle \smile}{}}.$$

After a bit of experimentation with these identifications, one discovers some fine features. The manipulations are equivalent to continuous deformations of lines in a plane [16]: Since $\delta_A^C \epsilon_{CD} \epsilon^{DE} \delta_E^B = \epsilon_{AD} \epsilon^{DB} = -\delta_A^B$, we have

$$\overset{\mathbf{B}}{\underset{\mathbf{A}}{\mathcal{N}}} = \overset{\mathbf{B}}{\underset{\mathbf{A}}{\big)}}.$$

Exercise 1. *Show that*

$$\overset{\frown}{\underset{\mathbf{A}\ \mathbf{B}}{\frown}} = \overset{\frown}{\underset{\mathbf{A} \quad \mathbf{B}}{}}$$

using a product of ϵ's.

On account of the relation $\delta_A^C \delta_B^D \tilde{\epsilon}_{CD} = -\tilde{\epsilon}_{AB}$ one has (The indices C and D are added to the diagram for clarity.)

$$\underset{\mathbf{A} \quad \mathbf{B}}{\overset{C \quad D}{\bowtie}} = -\overset{\frown}{\underset{\mathbf{A} \quad \mathbf{B}}{}}$$

– not what one would expect for smooth deformations of lines in a plane. This problem can be cured by associating a minus sign to each crossing. Thus by associating an i to every ϵ and a sign to every crossing, the diagrams behave as lines in the plane [16]. The more precise name of this concept is known as planar isotopy. Structures which can be moved about in this way are called topological. This association of curves to δ's and $\tilde{\epsilon}$'s allows one to perform algebraic calculations by moving lines in a plane.

A number of properties follow from the above definitions. The value of a simple closed loop takes a negative value[2]

$$(5) \qquad\qquad\qquad \bigcirc = -2,$$

since $\tilde{\epsilon}_{AB}\tilde{\epsilon}^{AB} = -\epsilon_{AB}\epsilon^{AB} = -2$. A closed line is a number. This turns out to be a generic result in that a spin network which has no open lines is equivalent to a number.

A surprisingly rich structure emerges when crossings, are considered. For instance the identity, often called the "spinor identity," links a pair of epsilons to products of deltas

$$\epsilon_{AC}\,\epsilon^{BD} = \delta_A^B\,\delta_C^D - \delta_A^D\,\delta_C^B.$$

Exercise 2. *Using the definitions of the $\tilde{\epsilon}$ matrices show that, diagrammatically, this becomes*

$$(6) \qquad\qquad \overset{\mathbf{B}\ \ \mathbf{D}}{\underset{\mathbf{A}\ \ \mathbf{C}}{\smile\!\!\frown}} + \underset{\mathbf{A}\ \ \mathbf{C}}{\overset{\mathbf{B}\ \ \mathbf{D}}{\bowtie}} + \overset{\mathbf{B}\ \ \mathbf{D}}{\underset{\mathbf{A}\ \ \mathbf{C}}{\big)\big(}} = 0.$$

---

[2]This led Penrose to dub these "negative dimensional tensors" [16]. In general relativity, the dimension of a space is given by the trace of the metric, $g_{\mu\nu}g^{\mu\nu}$, hence the name.

Note the sign changes, e.g. $-\delta_A^D \delta_C^B$ becomes $+ \ltimes$. This diagrammatic relation of Eq. (6 is known as "skein relations" or the "binor identity." The utility of this relation becomes evident when one realizes that the equation may be applied anywhere within a larger diagram.

The result of these associations is a topological structure in which algebraic manipulations of δ's, ϵ's, and other 2×2 matrices are encoded in manipulations of open or closed lines.

Exercise 3. *Show that the diagrammatics introduced in this section satisfy the Reidemeister Moves (see the appendix) and thus are topologically invariant.*

3.2. **Diagrams for angular momentum states.** This method expresses states such as $\mid jm \rangle$ and operators such as $\hat{J}^2$ in terms of diagrams. The notations are related as

$$\mid \tfrac{1}{2}\ \tfrac{1}{2} \rangle = u^A = \delta_1^A \sim \overset{A}{\underset{1}{\big|}} \ \text{ and}$$

$$\mid \tfrac{1}{2}\ -\tfrac{1}{2} \rangle = d^A = \delta_0^A \sim \overset{A}{\underset{0}{\big|}} \ .$$

These objects are like vectors, only a bit more simple. The vector index A takes values 0 or 1 only. (Secretly, the "u" for "up" tell us that the index A only takes the value 1. Likewise "d" tells us the index is 0.) The inner product is given by linking upper and lower indices, for instance

$$\langle \tfrac{1}{2}\ \tfrac{1}{2} \mid \tfrac{1}{2}\ \tfrac{1}{2} \rangle \sim \overset{l}{\underset{l}{\big|}} \ = 1.$$

This new diagram means that two of the diagrams $\big|$ are tied together with a Kroneker delta, $u^A u_B \delta_A^B$. For higher representations [14]

$$(7) \qquad \mid j\ m \rangle := \mid r\ s \rangle = N_{rs}\ \underbrace{u^{(A} u^B \ldots u^C}_{r}\ \underbrace{d^D d^E \ldots d^{F)}}_{s}$$

in which

$$(8) \qquad N_{rs} = \left(\frac{1}{r!\,s!\,(r+s)!} \right)^{1/2}, \quad j = \tfrac{r+s}{2}, \quad \text{and}\ \ m = \tfrac{r-s}{2}.$$

The parentheses in Eq. (7) around the indices indicate symmetrization, e.g. $u^{(A} d^{B)} = u^A d^B + u^B d^A$. The normalization N_{rs} ensures that the states are orthonormal in the usual inner product for $\mid jm \rangle$.

Multiple strands require multiple copies. The simplest example is for two lines

$$(9) \qquad \overset{|}{\underset{|}{2}} \ = \frac{1}{2} \left(\ \big)\big(\ -\ \asymp \ \right).$$

For more than two lines the idea is the same. One sums over permutations of the lines, adding a sign for each crossing. The general definition is

$$(10) \qquad \overset{|}{\underset{|}{n}} \ := \frac{1}{n!} \sum_{\sigma \in S_n} (-1)^{|\sigma|}\ \boxed{\begin{smallmatrix} \ldots n \ldots \\ \sigma_k \end{smallmatrix}}$$

in which a σ represents one permutation of the n lines and $|\sigma|$ is the minimum number of crossings for this permutation. The boxed σ in the diagram represents the action of the permutation on the lines. It can be drawn by writing $1\,2\,\ldots\,n$, then permutation just above it, and connecting the same elements by lines.

In this definition, the label n superimposed on the edge record the number of "strands" in the edge. Edge are usually labeled this way, though I will leave simple 1-lines unlabeled. Two other notations are used for this are

$$\underset{n}{|} \; = \; \underset{n}{+} \; = \; \boxed{...\,n\,...} \; .$$

The antisymmetrizers have a couple of lovely properties, retracing and projection. The antisymmetrizers are "irreducible," or vanish when a pair of lines is retraced

(11)
$$\boxed{\,...\,\cap\,...\,} = 0.$$

which follows from the antisymmetry. Using this and the binor identity of Eq. (6) one may show that the antisymmetrizers are "projectors" (the combination of two is equal to one)

$$\overset{+}{\underset{+}{_n}} \; = \; \underset{n}{|} \; .$$

Exercise 4. *Show this for a 2-line, i.e multiply (vertical composition) two copies of the right hand side of Eq. (9) and simplify using the skein relations (Eq. (6)) to show that only one copy remains.*

Making the simplest closed diagram out of these lines gives the loop value often denoted as Δ_n

$$\bigcirc{}_n \; = \Delta_n = (-1)^n (n+1).$$

The factor $n+1$ expresses the number of the "multiplicity" or the number of possible "A-values" on the edge: Each line in the edge carries an index, which takes two possible values. For an edge with a strands the sum of the indices $A, B, C, ...$ is $0, 1, 2, ..., a$. So that the sum takes $a+1$ possible values. One can show using the recursion relations for $\Delta_n{}^3$ that the loop value is equal to the multiplicity. But this is a longer argument. As we will see in the number of possible combinations is the dimension of the representation.

Exercise 5. *Show that the 2-loop has value 3, $\Delta_2 = 3$, using the relations for the basic loop value (Eq. (5)) and the expansion of the 2-line using the skein relation*

(12)
$$\underset{2}{|} \; = \; \Big)\Big(\; + \tfrac{1}{2} \; \underset{\cap}{\cup} \; .$$

These lines may be further joined into networks by making use of vertices. The trivalent vertex is defined as

$$\overset{a\quad b}{\underset{c}{\curlyvee}} \; := \; \overset{a\quad j\quad b}{\underset{c}{\mathord{\raise2pt\hbox{i}}\;k}} \; .$$
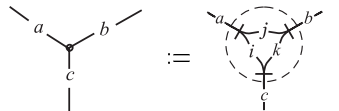
The dashed circle is a magnification of the dot in the diagram on the left. Such dashed curves indicate spin network structure at a point. The "internal" labels i, j, k are positive integers determined by the external labels a, b, c via

$$i = (a + c - b)/2, \quad j = (b + c - a)/2, \quad \text{and} \quad k = (a + b - c)/2.$$

As in quantum mechanics, the external labels must satisfy the triangle inequalities

$$a + b \geq c, \quad b + c \geq a, \quad a + c \geq b$$

and the sum $a + b + c$ is an even integer. These relations can be seen by drawing the strands through the vertex.

---

[3]The loop value satisfies $\Delta_0 = 1, \Delta_1 = -2$, and $\Delta_{n+2} = (-2)\Delta_{n+1} - \Delta_n$.

A useful representation of angular momentum states is in terms of the trivalent vertex. Using the notation $\bigwedge$ for many strands all labeled with 1 and similarly for d one has

$$| j\, m \rangle \sim \quad \text{[diagram]}$$

Note that the index on the open line (which I have not included) is a set of $r + s$ indices, r of which are 1 and s of which are 0. This is another way of writing the single index m.

Angular momentum operators also take a diagrammatic form. As all spin networks are built from spin-$\frac{1}{2}$ states, it is worth exploring this territory first. Spin-$\frac{1}{2}$ operators have a representation in terms of the Pauli matrices

$$\sigma_1 = \begin{pmatrix} 0 & 1 \\ 1 & 0 \end{pmatrix},\ \sigma_2 = \begin{pmatrix} 0 & -i \\ i & 0 \end{pmatrix},\ \sigma_3 = \begin{pmatrix} 1 & 0 \\ 0 & -1 \end{pmatrix}$$

with

$$\hat{S}_i = \frac{\hbar}{2}\sigma_i$$

for $i = 1, 2, 3$. Using the notation $|+\rangle$ for $|\frac{1}{2}\frac{1}{2}\rangle$ one has

$$\frac{\sigma_3}{2} |+\rangle = \tfrac{1}{2} |+\rangle,$$

which is expressed diagrammatically as

$$\text{[diagram]} = \tfrac{1}{2}\ \text{[diagram]} .$$

Or, since Pauli matrices are traceless,

$$\text{[diagram]} = 0,$$

and using Eq (12) one has

$$\text{[diagram]} = \tfrac{1}{2}\ \text{[diagram]} .$$

A similar relation holds for the states $|-\rangle$. The basic action of the spin operators can be described as a "hand" which acts on the state by "grasping" a line [19]. The result, after using the diagrammatic algebra, is either a multiple of the same state, as for σ_3, or a new state. If the operator acts on more than one line, a higher dimensional representation, then the total action is the sum of the graspings on each edge.[4]

Exercise 6. *(NB: A bit more than an exercise!) This form of the Pauli matrices also provide the needed foundation for the basic operations in quantum computing. This is also the basis for a diagrammatic programming language! Try constructing the NOT and Controlled NOT gates.*

---

[4]This may be shown by noticing that

$$\text{[diagram]} = \text{[diagram]}\ ,\ \text{so that}\ \text{[diagram]} + \text{[diagram]} + \cdots = n\ \text{[diagram]}\ ,$$

as may be derived using Eqs. (6) and (11).

The $\hat{J}_z$ operator can be constructed out of the σ_3 matrix. The total angular momentum z-component is the sum of individual measurements on each of the sub-systems; the operator is $\hat{J}_z = \hbar \sum_{i=1}^{2j+1} 1 \otimes \dots \otimes \left(\frac{\sigma_3}{2}\right)_i \otimes \dots \otimes 1$ where the sum is over the possible positions of the Pauli matrix. In diagrams, the action of the $\hat{J}_z$ operator becomes

$$\hat{J}_z \mid j\,m\rangle =$$

$$= r$$

$$= \hbar \left(\frac{r}{2} - \frac{s}{2}\right)$$

$$= \hbar\, m \mid j\,m\rangle .$$

The definition of the quantities r and s was used in the last line.

This same procedure works for the other angular momentum operators as well. The $\hat{J}_x$ operator is constructed from the Pauli matrix σ_1. When acting on one line the operator $\hat{J}_x$ matrix "flips the spin" and leaves a factor

$$\boxed{J_x} = \hbar\tfrac{1}{2}$$

Exercise 7. *Try the same procedure for $\hat{J}_y$.*

The raising and lowering operators are constructed with these diagrams as in the usual algebra. For the raising operator $\hat{J}_+ = \hat{J}_1 + i\hat{J}_2$ one has

$$\hat{J}_+ \mid j\,m\rangle = \hbar s$$

In a similar way one can compute

$$\hat{J}_- \hat{J}_+ \mid j\,m\rangle = \hbar^2 (r+1)s \mid j\,m\rangle$$

from which one can compute the normalization of these operators: Taking the inner product with $\langle j\,m \mid$ gives the usual normalization for the raising operator

$$\hat{J}_+ \mid j\,m\rangle = \hbar\sqrt{s\,(r+1)} \mid j\,m\rangle = \hbar\sqrt{(j-m)(j+m+1)} \mid j\,m\rangle .$$

Note that since r and s are non-negative and no larger than $2j$, the usual condition on m, $-j \leq m \leq j$, is automatically satisfied.

Though a bit more involved, the same procedure goes through for the $\hat{J}^2$ operator. It is built from the sum of products of operators $\hat{J}^2 = \hat{J}_x^{\,2} + \hat{J}_y^{\,2} + \hat{J}_z^{\,2}$. Acting once with the appropriate Pauli operators, one finds

$$\hat{J}^2 \mid j\,m\rangle = \hbar\frac{\hat{\sigma}_1}{2}\left[\frac{r}{2} \quad + \frac{s}{2} \right] + \hbar\frac{\hat{\sigma}_2}{2}\left[\frac{ir}{2} \quad - \frac{is}{2} \right]$$

$$+ \hbar\frac{\hat{\sigma}_3}{2}\frac{(r+s)}{2} \qquad .$$

Acting once again, some happy cancellation occurs and the result is

$$\hat{J}^2 \mid j\,m\rangle = \frac{\hbar^2}{2}\left(\frac{r^2+s^2}{2} + rs + r + s\right)\mid j\,m\rangle$$

which equals the familiar $j(j+1)$. Actually, there is a pretty identity which gives another route to this result. The Pauli matrices satisfy the magical relation

(13) $$\frac{1}{2}\sum_{i=1}^{3}\sigma^B_{i\,A}\,\sigma^D_{i\,C} = \frac{1}{2}\left(\delta^B_A\,\delta^D_C - \epsilon_{AC}\,\epsilon^{BD}\right) \equiv \ \substack{\mathbf{B} \\ \ }\!\!\succ\!\!-2\!\!-\!\!\prec\!\!\substack{\mathbf{D} \\ \ }$$

so the product is a 2-line. Similarly, the $\hat{J}^2$ operator may be expressed as a 2-line. As will be shown in Section (4) this simplifies the above calculation considerably.

4. A QUANTUM DESCRIPTION OF GEOMETRY

Now we have all the tools in place to describe quantum geometry, a diagrammatic algebra and the familiar $\hat{J}$ operators of angular momentum. A state of quantum gravity is given by a graph - a set of vertices and edges connecting them. To every edge of the graph we associate an angular momentum state and so a spin j. Finally, at the vertices – just as we do in spin-orbit coupling – the angular momenta of the incident edges are summed together. These three quantities, a graph, edge labels, and vertex labels define a "spin network."[5] These spin networks are "good quantum numbers" for the states. At an instant of time, quantum three dimensional space is represented by these graphs and labels. The edges may be all knoted together. The dynamics provides a way to chnage this "knotyness." As Shakespeare wrote in *Twelfth Night* "O time, thou must untangle this, not I, It is too hard a knot for me t'untie" (Viola).

I have not derived that spin networks form a basis, but rather stated the result. You might be (rightly) skeptical. So I must offer some motivation for this. We might expect that a quantum description of continuous geometry ought to be discrete (pun intended!).[6] But one can see how this comes out of the quantization.

In general relativity the degrees of freedom are encoded in the metric on space-time. However, it is quite useful to use different variables to quantize the theory [2]. Instead of a metric, in the Hamiltonian approach the variables are an "electric field," which is the "square root" of the spatial metric, and a vector potential. The electric field $\mathbf{E}$ is not only vector but also takes 2×2 matrix values in an "internal" space. This electric field is closely related to the coordinate transformation from curved to flat coordinates (a triad). The canonically conjugate $\mathbf{A}$, usually taken to be the configuration variable, is similar to the vector potential in electromagnetism but is more appropriately called a "matrix potential" for $\mathbf{A}$ also is matrix valued. It determines the effects of geometry on spin-$\frac{1}{2}$ particles as they travel about space.[7] (See Refs. [3] and [20] for more on the new variables.) States of loop quantum gravity are functions of the potential $\mathbf{A}$. A convenient basis is built from kets $\mid s\rangle$ labeled by spin networks s. In this application of spin networks, they have special tags or weights on the edges of the graph. Every strand e of the gravitational spin network has the "phase" $\int_e \mathbf{A} \cdot d\mathbf{l}$ associated to it. An orientation along every edge

---

[5]These objects were first invented by Roger Penrose to construct a discrete model of space [16].

[6]In a continuous space, in every interval there is an infinite number of points. Suppose that we are trying to specify the gravitational field in a region. If the theory associates 2 degrees of freedom per point, as general relativity does, and if this information requires some energy to store then the region would collapse into a black hole. This is a gravitational ultra-violet catastrophe. One solution to this is to remove the assumption of a continuous space.

[7]For those readers familiar with general relativity the potential determines the parallel transport of spin-$\frac{1}{2}$ particles.

helps to determine these phases or weights. The states of quantum geometry are encoded in the knottedness and connectivity of the spin networks.[8]

On this kinematical state space we have operators which measure the geometry, such as area. In calculus we calculate an area by integrating over a region R

$$\int_R d^2x$$

Hiding in this integral is a strong assumption – that the space is flat. For better or for worse, the region might contain some curvature. In this case the calculation is the same but there is a further dependence on the coordinates via the metric. Thus, the area of a surface is the integral

$$A_S = \int_S d^2x\sqrt{g},$$

in which g is the determinant of the metric on the surface. The flavor of this sort of thing is already familiar in flat space integrals in spherical coordinates:

$$A = \int r^2 \sin(\theta) d\phi d\theta.$$

In the $(\mathbf{A}, \mathbf{E})$ variables the calculation is more simple when the surface is specified by $z = 0$ in an adapted coordinate system. Expressed in terms of $\mathbf{E}$, the area of a surface S only depends on the z-vector component [17], [8], [4]

$$(14) \qquad\qquad A_S = \int_S d^2x\sqrt{E_z \cdot E_z}.$$

The dot product is in the "internal" space. It is the same product between Pauli matrices as appears in Eq. (13). In the spin network basis $\mathbf{E}$ is the momentum operator. As $p \to -i\hbar\frac{d}{dx}$ in quantum mechanics, the electric field becomes a hand, $\mathbf{E} \to -i\hbar\chi$ ⊤—2—• . The τ is proportional to a Pauli matrix, $\tau = \frac{i}{2}\sigma$ and the χ is a sign factor. It is positive when the orientations on the edge and surface are the same, negative when the edge is oriented oppositely from the surface, and vanishes when the edges is tangent to the surface. It turns out that the $\mathbf{E}$ operator is like the angular momentum operator $\hat{J}$, $\hat{\mathbf{E}} = \chi\hat{J}$! Since the $\mathbf{E}$ operator vanishes unless it grasps an edge, the operator only acts where the spin network intersects the surface.

The square of the area operator is calculated first. Calling the square of the integrand of Eq. (14) $\hat{O}$, the two-handed operator at one intersection is

$$(15) \qquad\qquad \hat{O} \mid s\rangle = -\sum_{e_I, e_J} \chi_I \chi_J \hat{J}_I \cdot \hat{J}_J \mid s\rangle$$

where the sum is over edges e_I at the intersection. Here, $\hat{J}_I$ denotes the vector operator $\hat{J} = \hat{J}_x + \hat{J}_y + \hat{J}_z$ acting on the edge e_I. This $\hat{O}$ is almost $\hat{J}^2$ but for the sign factors χ_I.

In the quantum theory, the integral of the area of a surface Eq. (14) is partitioned into small bits of area – as in the definition of integrals in calculus – which have only one intersection with the spin network state. The area operator then is the sum over contributions from all parts of the spin network which thread through the surface. In terms of $\hat{O}$ acting at all intersections i

$$(16) \qquad\qquad \hat{A}_S \mid s\rangle := \frac{G}{4c^3} \sum_i \hat{O}_i^{1/2} \mid s\rangle.$$

---

[8]In more detail, every edge has a holonomy or path ordered exponential (i.e. $\mathcal{P}\exp\int_e dt\,\dot{\mathbf{e}}(t) \cdot \mathbf{A}(e(t))$) associated to it. See, for example, Ref. [3].

FIGURE 1. Two types of intersections of a spin network with a
surface (a.) One isolated edge e intersects the surface transversely.
The normal $\hat{n}$ is also shown. (b.) One vertex of a spin network lies
in the surface. All the non-tangent edges contribute to the area.
Note that the network can be knotted.

One can calculate the action of the operator $\hat{O}$ on an edge e labeled by n as
depicted in Figure 4(a.). In this case, the hands act on the same edge so the sign
is 1, $\chi_I^2 = 1$, and the operator becomes $\hat{J}^2$. The calculation makes use of the Pauli
matrix identity of Eq. (13)

$$\hat{O}_e \mid s\rangle = -\hat{J}^2 \mid s\rangle$$

$$= -\hbar^2 \, \frac{n^2}{2} \; \text{⬡} \; \mid (s - e)\rangle.$$

The edge is shown in the the diagram so it is removed spin network s giving the
state $\mid (s - e)\rangle$. Now the diagram may be reduced using the diagram identities.
The bubble may be extracted with Eq. (22)

$$\hat{O}_e \mid s\rangle = -\hbar^2 \, \frac{n^2}{2} \; \text{⬡} \; \mid (s - e)\rangle$$

$$= -\hbar^2 \, \frac{n^2}{2} \, \frac{\theta(n, n, 2)}{\Delta_n} \; \text{⬡} \; \mid (s - e)\rangle$$

$$= -\hbar^2 \, \frac{n^2}{2} \left(-\frac{n + 2}{2n} \right) \mid s\rangle$$

$$= \hbar^2 \, \frac{n(n + 2)}{4} \mid s\rangle,$$

in which Eq. (21) was also used in the second line. Putting this result into the area
operator, one learns that the area coming from all the transverse edges is [17]

(17)
$$\hat{A}_S \mid s\rangle = \frac{G\hbar}{c^3} \sum_i \sqrt{\frac{n_i(n_i + 2)}{4}} \mid s\rangle$$

$$= l_p^2 \sum_i \sqrt{j_i(j_i + 1)} \mid s\rangle.$$

The units $\hbar, c$, and G are collected into the Planck length $l_p = \sqrt{\frac{G\hbar}{c^3}} \sim 10^{-35}$ m.
The result is also re-expressed in terms of the more familiar angular momentum
variables $j = \frac{n}{2}$.

The full spectrum of the area operator is found by considering all the intersections
of the spin network with the surface S including vertices which lie on the surface
as in Figure 4(b.). The edges incident to a vertex on the surface are divided into
three categories, those which are above the surface j^u, below the surface j^d, and
tangent to the surface j^t. Summing over all contributions [4]

$$\hat{A}_S \mid s\rangle = \frac{l_P^2}{2} \sum_v \left[2j_v^u(j_v^u + 1) + 2j_v^d(j_v^d + 1) - j_v^t(j_v^t + 1) \right]^{1/2} \mid s\rangle.$$

This result is utterly remarkable in that the calculation predicts that space is discrete. Measurements of area can only take these quantized values. As is the case in many quantum systems there is a "gap" from zero to the lowest possible non-zero value. This area gap is

$$(18) \qquad \Delta A_0 = \frac{\sqrt{3}}{4} l_p^2.$$

In an analogous fashion, as for an electron in a hydrogen atom, surfaces make a quantum jump between states in the spectrum of the area operator; there is a quanta of area.

Now we can return to the question of black hole radiation.

4.1. **Spectra of black hole radiation.** Suppose that the most likely configuration for a black hole is one with many, many ($\sim 10^{70}$) edges intersecting the boundary each carrying the simplest representation $j = 1/2$. To reduce the area of the horizon, a black hole must loose an edge intersecting the horizon - pop! The area of the horizon makes a quantum jump and radiates like an atom. This smallest transition determines the fundamental frequency of a black hole [6].

From Eq. (2) we have that, for a Schwarschild black hole,

$$M^2 = \frac{c^4}{16\pi G^2} A_{\mathcal{H}}$$

so that the change in mass is

$$\Delta M = \frac{c^4}{32\pi G^2} \frac{1}{M} \Delta A_{\mathcal{H}}.$$

Using the change in area ΔA_0 of Eq. (18), the fundamental frequency ω_0 is

$$\omega_0 = \frac{\sqrt{3}}{64\pi} \frac{c^3}{G} \frac{1}{M} \approx 1.7 \times 10^3 \left(\frac{M_\odot}{M} \right) \text{Hz}$$

For example, if the black hole has an effective mass of one solar mass then ω_0 is on the order of kHz – stellar mass black holes emit *radio* waves [21]!

To find whether this frequency is small in scale relative to the body body spectrum, one can find the maximum of the spectrum. The maximum is located at $\hbar \omega / kT \sim 3$ so the frequency of the maximum is

$$\omega_{max} \sim \frac{3kT_H}{\hbar} = \frac{3c^3}{8\pi GM} \approx 14\omega_0.$$

The maximum of the Planck distribution is just 14 times the fundamental frequency! This is radically different than the Hawking spectrum. Though both spectra would fit in the same envelope, there would only be about 30 visible lines for all black holes, independent on the mass.

These results are for the spectrum of a spherically symmetric black hole. One could expect that the spectrum of real black holes would be significantly modified by transitions between various angular momentum states. As in atomic physics, these transitions, emission or absorption of gravitons or photons, give fine structure. However, as long as these transitions between discrete angular momentum states are small compared to the irreducible mass squared, the blurring of the black hole emission lines is small compared to the fundamental wavelength ω_0^{-1} [5].

There is an unfortunate aspect of these larger black holes. The power radiated, as it scales as T_H^4, is fantastically small. So it is not likely that this effect could be observed. This calculation is too simple in another regard as well. The assumption that $\Delta A = \frac{\sqrt{3}}{4} l_p^2$ may not be true. In fact, the level spacing of the spectrum decreases with increasing spin. In these cases, the semiclassical Hawking spectrum is reproduced [3].

4.2. **Traces of discrete structure.** A discrete structure such as spin networks could yield observable affects. One possibility is through a small modification of Maxwell's equations. As in optical media such as crown or flint glass, a quantum gravitational medium would respond differently to the propagation of particles at different wavelengths or energies. This would be a very small effect but over vast distances, the result could be measurable.

Let's look at how this would work for photons [1]. For a theory at a scale E_{QG}, the effect would be realized by a modification of the speed of light

$$v(E) = c \left(1 + \alpha \frac{E}{E_{QG}} + \beta \left(\frac{E}{E_{QG}} \right)^2 + \ldots \right)$$

so that photons with different energies E would travel at different speeds. In optics we normally encode this change as the index of refraction n; $v_{medium} = \frac{c}{n}$. For $v(E)$,

$$n = \frac{1}{1 + \alpha \frac{E}{E_{QG}}}.$$

If a bundle of photons were released simultaneously over a wide range of energy, the photons would arrive at their destination, say a distance L from the source, at different times. The first order delay can be found to be

(19) $$\Delta t \approx \alpha \frac{L}{c} \frac{\Delta E}{E_{QG}}.$$

Though the effect $(\frac{E}{E_{QG}})$ is tiny, if the distances are astronomical then the effect could be observed. It was suggested last year [1], that the current γ-ray observations *already* place limits on the scale of this effect up to $E_{QG} > 10^{16}$ GeV.

How could this be done? The idea is that it the signal has a fine enough time structure, a detailed time-series analysis comparing signals in different energy bands might reveal coincidences on a time scale of $\Delta t \sim 10^{-2}$. If the sources are at $L \sim 10^{10}$ l.yr. and since the energy resolution of the BATSE detector on the Compton Observatory is $\Delta E \sim 200$ keV, then Eq. (19) constrains the energy scale E_{QG} of quantum gravity dispersive effects. In principle, one could do much better. Gamma ray sources have photons in the 0.1 - 100 MeV range (with some possibility of photons in the Tev range) with time scale features on the order of 10^{-3} s. There is also a possibility of polarization effects such a birefringence as well [9].

How could we distinguish this from regular dispersive effects? The key property of this dispersion is that, unlike normal dispersion,

$$\frac{dn_{QG}}{d\lambda} > 0,$$

the index of refraction decreases as the wavelength decreases.

This being a cumulative effect, signals traveling over a vast distance would develop traces of the underlying discrete structure.

Exercise 8. *(NB: A bit more than an exercise!) For a realistic spin network model of flat space, find the dispersion relation for massless particle propagation.*

5. Conclusions

This talk on quantum gravity offers a view of issues surrounding the formulation of such a theory, a glimpse of the structure of spin network geometry, and two avenues for experimental observations.

But I do not want to leave you without a note of caution, which also may tickle your imagination. This comment relates to the thermodynamical relations

I mentioned before which was that general relativity plus some quantum theory reproduced thermodynamics.

Let me quote from a statistical mechanics text, "The thermodynamic laws, then, are introduced only as phenomenological statements that conveniently summarize macroscopic experience. ... we introduce thermodynamic laws, which may be regarded as mathematical axioms defining a mathematical model. It is possible to deduce rigorous consequences of these axioms, but it is important to remember that this model may not rigorously correspond to the physical world;" [11]

In the first section of the talk I briefly reviewed how general relativity plus quantum theory gives thermodynamics. Does this not suggests that, "General relativity is the phenomenology of geometry" ?! Does Einstein's work "conveniently summarize macroscopic experience"?

Exercise 9. *(NB: A bit more than an exercise!) What is the statistical mechanics of spacetime geometry?*

We may have to come up with a far more radical theory than either general relativity or quantum theory. When Dirac first tried to find a (special) relativistic equation for the electron he asked for an equation that simultaneously satisfied the principles of special relativity and quantum mechanics, he found a new "internal" degree of freedom. This is the fully-quantum "spin" of particles. Spin has profound consequences from stellar evolution to high school chemistry (with the formation of life in between!). Our world would not be recognizable without this quantum phenomenon. So just as when Dirac, faced with the seemingly incompatible requirements of special relativity and quantum theory pushed hard, played a clever trick, and discovered spin, there is no reason to expect that quantum gravity will lead to physical phenomenon less profound. At least, I hope to leave you with our eyes open to this possibility.

Appendix A. Loops, Thetas, Tets and all that

This appendix contains the basic definitions and formulae of diagrammatic recoupling theory using the conventions of Kauffman and Lins [13], a book written in the context of the more general Temperley-Lieb algebra. It also includes a description of the Reidemeister Moves of knot theory.

A.1. **Reidemeister Moves.** It is remarkable that a knot in three dimensional space can be continuously deformed into another knot, if and only if, the planar projection of the knots can be transformed into each other via a sequence of four moves called the "Reidemeister moves" [18]. Though I discuss only two dimensional diagrams here, the Reidemeister moves are shown in their full generality – as projections of knots in three dimensional space. While in two dimensions one has only an intersection, $\times$, when two lines cross, in three dimensions one has the "over crossing," $\times$ and the "undercross," $\times$, as well as the intersection $\times$.

There are four moves:

- **Move 0:** In the plane of projection, one can make smooth deformations of the curve

$$ \mathcal{N} \sim | \; . $$

- **Move I:** As these moves are designed for one dimensional objects, a curl may be undone
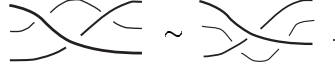
$$ \mathcal{G} \sim | \; . $$

This move does not work on garden-variety string. The string becomes twisted (or untwisted). (In fact, this is the way yarn is made.)

- **Move II:** The overlaps of distinct curves are not knotted

$$\text{(diagram)} \quad \sim \quad \text{(diagram)} \ .$$

- **Move III:** One can perform planar deformations under (or over) a diagram

$$\text{(diagram)} \quad \sim \quad \text{(diagram)} \ .$$

With a finite sequence of these moves the projection of a knot may be transformed into the projection of any other knot which is topologically equivalent to the original. If two knots may be expressed as the other with a sequence of these moves then the knots are called "isotopic." Planar isotopy is generated by all four moves with the significant caveat that there are no crossings $\times$, only intersections $\times$. Planar isotopy may be summarized as the manipulations one would expect for elastic, non-sticky strings on a table top – if they are infinitely thin.

Move I on real strings introduces a twist in the string. This move is violated by any line which has some spatial extent in the transverse direction such as ribbons. Happily, there are diagrammatic spin networks for these "ribbons" as well [12], [13].

A.2. **Diagrammatic Formulae.** The function $\theta(m,n,l)$ is given by

$$(20) \qquad \theta(m,n,l) = \text{(diagram)} = (-1)^{(a+b+c)} \frac{(a+b+c+1)!\,a!\,b!\,c!}{(a+b)!\,(b+c)!\,(a+c)!}$$

where $a = (l+m-n)/2$, $b = (m+n-l)/2$, and $c = (n+l-m)/2$. An evaluation which is useful in calculating the spectrum of the area operator is $\theta(n,n,2)$, for which $a = 1$, $b = n-1$, and $c = 1$.

$$(21) \qquad \theta(n,n,2) = (-1)^{(n+1)} \frac{(n+2)!\,(n-1)!}{(2n!)^2} = (-1)^{(n+1)} \frac{(n+2)(n+1)}{2n} \ .$$

A "bubble" diagram is proportional to a single edge.

$$(22) \qquad \text{(diagram)} = \delta_{nl} \frac{(-1)^n \theta(a,b,n)}{(n+1)} \ \Big|_n^{\ } \ .$$

Exercise 10. *Check the identity Eq. (22) by closing up the lines and applying the definitions of the loop value and θ.*

The basic recoupling identity relates the different ways in which three angular momenta, say a, b, and c, can couple to form a fourth one, d. The two possible recouplings are related by

$$(23) \qquad \text{(diagram)} = \sum_{|a-b| \le i \le (a+b)} \left\{ \begin{array}{ccc} a & b & i \\ c & d & i' \end{array} \right\} \text{(diagram)}$$

where on the right hand side is the $6j$-symbol defined below. It is closely related to the Tet symbol. This is defined by [13]

$$\text{(diagram)} = \text{(diagram)} = Tet \begin{bmatrix} a & b & e \\ c & d & f \end{bmatrix}$$

$$(24) \qquad Tet \begin{bmatrix} a & b & e \\ c & d & f \end{bmatrix} = N \sum_{m \le s \le S} (-1)^s \frac{(s+1)!}{\prod_i (s-a_i)! \prod_j (b_j - s)!}$$

$$N = \frac{\prod_{i,j} [b_j - a_i]!}{a!\,b!\,c!\,d!\,e!\,f!}$$

in which

$$a_1 = \tfrac{1}{2}(a+d+e) \qquad\qquad\qquad b_1 = \tfrac{1}{2}(b+d+e+f)$$
$$a_2 = \tfrac{1}{2}(b+c+e) \qquad\qquad\qquad b_2 = \tfrac{1}{2}(a+c+e+f)$$
$$a_3 = \tfrac{1}{2}(a+b+f) \qquad\qquad\qquad b_3 = \tfrac{1}{2}(a+b+c+d)$$
$$a_4 = \tfrac{1}{2}(c+d+f) \qquad m = \max\{a_i\} \quad M = \min\{b_j\}$$

The $6j$-symbol is then defined as

$$\left\{ \begin{array}{ccc} a & b & i \\ c & d & j \end{array} \right\} := \frac{Tet \begin{bmatrix} a & b & i \\ c & d & j \end{bmatrix} \Delta_i}{\theta(a,d,i)\,\theta(b,c,i)}.$$

These satisfy a number of properties including the orthogonal identity

$$\sum_l \left\{ \begin{array}{ccc} a & b & l \\ c & d & j \end{array} \right\} \left\{ \begin{array}{ccc} d & a & i \\ b & c & l \end{array} \right\} = \delta_i^j$$

and the Biedenharn-Elliot or Pentagon identity

$$\sum_l \left\{ \begin{array}{ccc} d & i & l \\ e & m & c \end{array} \right\} \left\{ \begin{array}{ccc} a & b & f \\ e & l & i \end{array} \right\} \left\{ \begin{array}{ccc} a & f & k \\ d & d & l \end{array} \right\} = \left\{ \begin{array}{ccc} a & b & k \\ c & d & i \end{array} \right\} \left\{ \begin{array}{ccc} k & b & f \\ e & m & c \end{array} \right\}.$$

Two lines may be joined via

(25) $$\quad = \sum_c \frac{\Delta_c}{\theta(a,b,c)} \quad .$$

One also has occasion to use the coefficient of the "λ-move"

(26) $$\quad = \lambda_c^{ab} \quad \text{where } \lambda_c^{ab} \text{ is}$$
$$\lambda_c^{ab} = (-1)^{[a^2+b^2-c^2]/2}.$$

REFERENCES

[1] G. Amelino-Camelia, J. Ellis, N.E. Mavromatos, D.V. Nanopoulos, and S. Sarkar, *Nature* **393** (1998) 763-765. See also Online eprint archive: *http://xxx.lanl.gov/abs/astro-ph/9810483*.

[2] Abhay Ashtekar, "New variables for classical and quantum gravity," *Phys. Rev. Lett.* **57**(18), 2244-2247 (1986); *New perspectives in canonical gravity* (Bibliopolis, Naples, 1988); *Lectures on non-perturbative canonical gravity*, Advanced Series in Astrophysics and Cosmology-Vol. 6 (World Scientific, Singapore, 1991).

[3] Abhay Ashtekar, "Quantum mechanics of Riemannian geometry," *http://vishnu.nirvana.phys.psu.edu/riem_qm/riem_qm.html*.

[4] Abhay Ashtekar and Jerzy Lewandowski, "Quantum Theory of Geometry I: Area operators," *Class. Quant. Grav.* **14**, A55-A81 (1997).

[5] J. Bekenstein, *Lett. Nuovo Cimento* **11** (1974) 467.

[6] J. Bekenstein and V. F. Mukanhov, *Phys. Lett.* **B 360** (1995) 7.

[7] Roberto De Pietri and Carlo Rovelli, "Geometry eigenvalues and the scalar product from recoupling theory in loop quantum gravity," *Phys. Rev. D* **54**(4), 2664-2690 (1996).

[8] S. Fittelli, L. Lehner, C. Rovelli, "The complete spectrum of the area from recoupling theory in loop quantum gravity," *Class. Quant. Grav.* **13**, 2921-2932 (1996).

[9] R. Gambini and J. Pullin, "Nonstandard optics from quantum spacetime." Online eprint archive: *http://xxx.lanl.gov/abs/gr-qc/9809038*.

[10] S. Hawking, *Nature* **248** (1974) 30; *Comm. Math. Phys* **43** (1974) 248.

[11] Kerson Huang, *Statistical Mechanics* (John Wiley, 1963) pp. 6-7.

[12] Louis H. Kauffman, *Knots and Physics*, Series on Knots and Everything - Vol. 1 (World Scientific, Singapore, 1991) pp. 125-130, 443-471.

[13] Louis H. Kauffman and Sóstenes L. Lins, *Temperley-Lieb Recoupling Theory and Invariants of 3-Manifolds*, Annals of Mathematics Studies N. 134, (Princeton University Press, Princeton, 1994), pp. 1-100.

[14] John P. Moussouris, "Quantum models as spacetime based on recoupling theory," Oxford Ph.D. dissertation, unpublished (1983).

[15] Miyoshi et al, *Nature* 373 (1995) 127.

[16] Roger Penrose, "Angular momentum: An approach to combinatorial spacetime" in *Quantum Theory and Beyond* T. Bastin, ed. (Cambridge University Press, Cambridge, 1971); "Combinatorial Quantum Theory and Quantized Directions" in *Advances in Twistor Theory*, Research Notes in Mathematics 37, L. P. Hughston and R. S. Ward, eds. (Pitman, San Francisco, 1979) pp. 301-307; "Theory of Quantized Directions," unpublished notes.

[17] Carlo Rovelli and Lee Smolin, "Discreteness of area and volume in quantum gravity," *Nuc. Phys.* **B 442**, 593-622 (1995).

[18] K. Reidemeister, *Knotentheorie* (Chelsea Publishing Co., New York, 1948), original printing (Springer, Berlin, 1932). See also Louis Kauffman, *Knots and Physics*, pp. 16.

[19] Carlo Rovelli and Lee Smolin, "Loop Representation of quantum general relativity," *Nuc. Phys.* **B 331**(1), 80-152 (1990).

[20] Carlo Rovelli, "Loop Quantum Gravity," *Living Reviews in Relativity* http://www.livingreviews.org/Articles/Volume1/1998-1rovelli; "Strings, Loops, and Others: A critical survey of the present approaches to quantum gravity," in *Gravitation and Relativity: At the turn of the Millennium*, Proceedings of the GR-15 Conference, Naresh Dadhich and Jayant Narlikar, ed. (Inter-University Center for Astronomy and Astrophysics, Pune, India, 1998), pp. 281 - 331, Online eprint archive: *http://xxx.lanl.gov/abs/gr-qc/9803024*.

[21] L. Smolin, *Matters of Gravity* **7** (1996) 10.

Institut für Theoretische Physik, Der Universität Wien, Boltzmanngasse 5, A-1090 Wien AUSTRIA

E-mail address: `smajor@galileo.thp.univie.ac.at`